

Effective action for Bose-Einstein condensates

Takafumi Kita

Department of Physics, Hokkaido University, Sapporo 060-0810, Japan

(Dated: January 16, 2022)

We clarify basic properties of an effective action (i.e., self-consistent perturbation expansion) for interacting Bose-Einstein condensates, where field ψ itself acquires a finite thermodynamic average $\langle\psi\rangle$ besides two-point Green's function \hat{G} to form an off-diagonal long-range order. It is shown that the action can be expressed concisely order by order in terms of the interaction vertex and a special combination of $\langle\psi\rangle$ and \hat{G} so as to satisfy both Noether's theorem and Goldstone's theorem (I) corresponding to the first proof. The self-energy is predicted to have a one-particle-reducible structure due to $\langle\psi\rangle \neq 0$ to transform the Bogoliubov mode into a bubbling mode with a substantial decay rate.

I. INTRODUCTION

Self-consistent approximations have played a crucial role for clarifying basic or exotic properties of diverse condensed matter systems. Lowest-order ones with respect to the interaction are generally known as mean-field or molecular-field theories, which already include many outstanding examples such as the Hartree-Fock approximation for normal states, Weiss and Stoner theories for ferromagnetism, and Bardeen-Cooper-Schrieffer theory for superconductivity. In general, the self-consistent scheme has a notable advantage over the simple perturbation expansion that spontaneous symmetry-breaking phases can be described on an equal footing.

This approach can be improved systematically to include higher-order correlations based on a self-consistent perturbation expansion with Matsubara Green's function,¹⁻⁵ as first shown by Luttinger and Ward for normal states.¹ Another advantage of this method is that it satisfies various conservation laws, i.e., Noether's theorem,⁶ as pioneered by Kadanoff and Baym⁷ and later shown unambiguously by Baym.⁸ Hence, it can be used to describe nonequilibrium phenomena, including their approach to equilibrium, by transforming the imaginary-time Matsubara contour into the real-time Schwinger-Keldysh contour.⁹⁻¹¹ Later, this “ Φ -derivable” or “conserving” approximation scheme has also been generalized to relativistic quantum field theory by Cornwall, Jackiw, and Tomboulis (CJT)¹² to find a wide field of applications in high-energy physics with the name of “two-particle-irreducible (2PI) effective action.”^{13,14}

However, extending this powerful formalism to Bose-Einstein condensates (BECs) has encountered a serious “conserving vs. gapless” dilemma that either Noether's theorem for conservation laws or Goldstone's theorem (I) for spontaneously broken symmetries is violated in standard approximations,^{6,15,16} as first pointed out by Hohenberg and Martin in 1965.^{17,18} The basic difficulty lies in how to renormalize the condensate wave function $\Psi \equiv \langle\psi\rangle$ and quasiparticle Green's function \hat{G} consistently in the presence of tadpole and other anomalous interaction vertices characteristic of BECs (see Fig. 2(b)-

(d) below) so as to satisfy the two fundamental theorems simultaneously.

It was shown in a previous paper⁴ that this long-standing problem may be resolved successfully by extending the Luttinger-Ward theory to BECs with the help of an identity for the interaction energy. The resultant formalism reveals that there should be a new class of Feynman diagrams for the self-energy that has been overlooked so far, i.e., those that may be classified as “one-particle reducible” (1PR) due to tadpole and other anomalous interaction vertices.¹⁹ The rationale for their existence is that they are indispensable for the identity to be satisfied order by order in the self-consistent perturbation expansion with respect to the interaction in the same way as the Luttinger-Ward functional. This novel structure of the self-energy has been predicted to modify standard results based on the Bogoliubov theory²⁰⁻²⁶ substantially. For example, we have pointed out in a previous paper²⁷ that it will add a term to the Lee-Huang-Yang expressions²¹ for the ground-state energy and condensate density of the dilute Bose gas; see Eq. (30) below for further details. We have also shown²⁸ that it will transform the single-particle Bogoliubov mode with an infinite lifetime into a bubbling mode with a considerable decay rate that is proportional to the s -wave scattering a in the dilute limit. Finally, this single-particle bubbling mode should be different in character from the two-particle collective excitation,^{19,29} contrary to the standard understanding where both are considered identical.²³⁻²⁶ Nevertheless, the two modes may be regarded separately as Nambu-Goldstone bosons corresponding to the two different proofs;^{6,15} their contents should be distinguished clearly as “Goldstone's theorem (I)” and “Goldstone's theorem (II)”¹⁹ with the former being identical to the Hugenholtz-Pines theorem.³⁰

Now, purposes of the present paper are twofold. First, we report a further refinement of this formalism, whose key quantity has been the Φ functional, $\Phi = \Phi[\Psi, \bar{\Psi}, \hat{G}]$, given as a power series of the interaction.⁴ We will show that it can be transformed into a functional $\Phi = \Phi[\hat{G}]$ of a single quantity \hat{G} that is defined in terms of \hat{G} , Ψ , and $\bar{\Psi}$ as Eq. (15) below. Thus, the condensate wave function apparently disappears from Φ , thereby resulting in a considerable reduction in the number of Feynman diagrams

to be considered. This fact will be checked specifically up to the forth order of the expansion with respect to the interaction. It will also be exemplified that any single diagram of the normal state can be a source of an approximate Φ for BECs that satisfies both Noether's theorem and Goldstone's theorem (I). Second, we will trace possible origins of a discrepancy between the present Φ with a one-particle-irreducible (1PI) structure and the one given by CJT,¹² which consists of 2PI diagrams that cannot be separated by cutting any pair of \hat{G} lines even for spontaneous symmetry-breaking phases of $\langle\psi\rangle \neq 0$.

In Sec. II, we transform results of the previous study⁴ into the Lagrangean formalism with path integrals. The discrepancy between the CJT¹² and present formalisms is discussed in Sec. II G in the context of Bose-Einstein condensation. In Sec. III, it will be shown that the Φ functional can be given concisely as a functional of \hat{G} defined by Eq. (15) below. Section IV provides a brief summary.

II. SUMMARY OF PREVIOUS RESULTS

A. System and basic quantities

We consider an ensemble of identical bosons with mass m and spin 0 described by the action^{6,31}

$$S = S_0 + S_{\text{int}}, \quad (1)$$

with

$$S_0 = \int d^4x \bar{\psi}(x) \left(\frac{\partial}{\partial \tau} - \frac{\hbar^2 \nabla^2}{2m} - \mu \right) \psi(x), \quad (2a)$$

$$S_{\text{int}} = \frac{1}{2} \int d^4x \int d^4y V(|x-y|) \bar{\psi}(x) \bar{\psi}(y) \psi(y) \psi(x). \quad (2b)$$

Here ψ is the complex bosonic field and $\bar{\psi}$ its conjugate, $x \equiv (\mathbf{r}, \tau)$ specifies a space-“time” point with $0 \leq \tau \leq \beta \equiv (k_B T)^{-1}$ (k_B : Boltzmann constant, T : temperature), μ is the chemical potential, and V is an interaction potential.

It is convenient to regard ψ and $\bar{\psi}$ as elements of a column or row vector as

$$\begin{bmatrix} \psi \\ \bar{\psi} \end{bmatrix} \equiv \begin{bmatrix} \psi_1 \\ \psi_2 \end{bmatrix} \equiv \vec{\psi}, \quad [\bar{\psi} \ \psi] \equiv [\psi^1 \ \psi^2] \equiv \vec{\psi}^\dagger, \quad (3)$$

so that $\psi^i = \psi_{3-i}$ ($i = 1, 2$). Next, we define the condensate wave function Ψ_i and a 2×2 matrix Green's function $\hat{G} \equiv (G_{ij})$ in the Nambu space by

$$\Psi_i(x) \equiv \langle \psi_i(x) \rangle, \quad (4a)$$

$$G_{ij}(x, y) \equiv [\langle T_\tau \psi_i(x) \psi^j(y) \rangle - \Psi_i(x) \Psi^j(y)] (-1)^j, \quad (4b)$$

which obeys $G_{ij}(x_1, x_2) = (-1)^{i+j-1} G_{3-j, 3-i}(x_2, x_1) = (-1)^{i+j} G_{ji}^*(\mathbf{r}_2 \tau_1, \mathbf{r}_1 \tau_2)$.^{4,29} With these symmetries, it is

convenient for later purposes to introduce

$$G(x, y') \equiv \bar{G}(y', x) \equiv \frac{G_{11}(x, y') - G_{22}(y', x)}{2}, \quad (5a)$$

$$F(x, y) \equiv \frac{G_{12}(x, y) + G_{12}(y, x)}{2}, \quad (5b)$$

$$\bar{F}(x', y') \equiv -\frac{G_{21}(x', y') + G_{21}(y', x')}{2}, \quad (5c)$$

where non-primed (primed) arguments are associated with ψ ($\bar{\psi}$). Function G is the conventional Green's function that remains finite in normal states, whereas F and \bar{F} are “anomalous” ones characteristic of the off-diagonal long-range order (ODLRO)³² with $\bar{F}(x'_1, x'_2) = F^*(\mathbf{r}'_2 \tau'_1, \mathbf{r}'_1 \tau'_2)$.

Inverse matrix of $\hat{G} = (G_{ij})$ for $V \rightarrow 0$ can be written explicitly in terms of the operators in Eq. (2a) as⁴

$$\hat{G}_0^{-1}(x, y) \equiv \left[-\hat{\sigma}_0 \frac{\partial}{\partial \tau} + \hat{\sigma}_3 \left(\frac{\hbar^2 \nabla^2}{2m} + \mu \right) \right] \delta(x - y), \quad (6)$$

where $\hat{\sigma}_0$ and $\hat{\sigma}_3$ denote the 2×2 unit matrix and third Pauli matrix, respectively.

It is also useful to introduce a symmetrized vertex as

$$V_s(x' y', xy) \equiv \frac{1}{2} V(|x-y|) [\delta(x', x) \delta(y', y) + \delta(x', y) \delta(y', x)]. \quad (7)$$

Using it, we can express Eq. (2b) alternatively as

$$S_{\text{int}} = \frac{1}{2} \int d^4x' \int d^4y' \int d^4x \int d^4y V_s(x' y', xy) \times \bar{\psi}(x') \bar{\psi}(y') \psi(y) \psi(x). \quad (8)$$

B. Legendre transformation

As shown by De Dominicis and Martin,² a Legendre transformation enables us to establish the stationarity of the grand potential with respect to $\vec{\Psi}$ and \hat{G} concisely and clearly. Let us introduce the grand partition function $Z[\vec{J}, \hat{K}]$ for action (1) with extra source functions $J^i(x) = J_{3-i}(x)$ and $K_{ij}(x, y) = K_{3-j, 3-i}(y, x)$ by^{2,6,31}

$$Z[\vec{J}, \hat{K}] \equiv \int D(\bar{\psi}, \psi) \exp \left[-S + \sum_i \int d^4x J^i(x) \psi_i(x) + \sum_{ij} \int d^4x \int d^4y \psi^j(y) K_{ji}(y, x) \psi_i(x) \right], \quad (9)$$

which satisfies

$$\frac{\delta \ln Z[\vec{J}, \hat{K}]}{\delta J^i(x)} = \Psi_i(x), \quad (10a)$$

$$\frac{\delta \ln Z[\vec{J}, \hat{K}]}{\delta K_{ji}(y, x)} = \langle T_\tau \psi_i(x) \psi^j(y) \rangle = G_{ij}(x, y) (-1)^j + \Psi_i(x) \Psi^j(y). \quad (10b)$$

Subsequently, we perform a Legendre transformation from $-\ln Z[\vec{J}, \hat{K}]$ to $\Gamma = \Gamma[\vec{\Psi}, \hat{G}]$ as

$$\begin{aligned} \Gamma[\vec{\Psi}, \hat{G}] \equiv & -\ln Z[\vec{J}, \hat{K}] + \sum_i \int d^4x J^i(x) \Psi_i(x) \\ & + \sum_{ij} \int d^4x \int d^4y K_{ij}(x, y) \langle T_\tau \psi_j(y) \psi^i(x) \rangle. \end{aligned} \quad (11)$$

It satisfies

$$\begin{aligned} \frac{\delta \Gamma[\vec{\Psi}, \hat{G}]}{\delta \Psi_i(x)} &= J^i(x) + 2 \sum_j \int d^4y \Psi^j(y) K_{ji}(y, x), \\ \frac{\delta \Gamma[\vec{\Psi}, \hat{G}]}{\delta G_{ji}(y, x)} &= (-1)^i K_{ij}(x, y). \end{aligned}$$

Especially for the cases of physical interest with $\vec{J} = \vec{0}$ and $\hat{K} = \hat{0}$, they are reduced to the stationarity conditions

$$\frac{\delta \Gamma[\vec{\Psi}, \hat{G}]}{\delta G_{ji}(y, x)} = 0, \quad \frac{\delta \Gamma[\vec{\Psi}, \hat{G}]}{\delta \Psi_i(x)} = 0. \quad (12)$$

The corresponding Γ is known as “quantum effective action” or simply “effective action” in relativistic quantum field theory.^{6,12} Note also that $\Omega[\vec{\Psi}, \hat{G}] \equiv \Gamma[\vec{\Psi}, \hat{G}]/\beta$ is the grand potential of thermodynamics. The first equality of Eq. (12) is exactly the stationarity condition established diagrammatically by Luttinger and Ward for normal states.¹

C. Exact results

As pointed out by Jona-Lasinio,¹⁶ partition function (9) for $\hat{K} \equiv \hat{0}$ and the corresponding $\Gamma = \Gamma[\vec{\Psi}]$ are useful for obtaining formally exact results for $\vec{J} \rightarrow \vec{0}$. First, one can show that Green’s function (4b) obeys the Dyson-Beliaev equation^{4,6,16,33}

$$\hat{G}^{-1} = \hat{G}_0^{-1} - \hat{\Sigma}, \quad (13a)$$

where $\hat{G}_0^{-1} = \hat{G}_0^{-1}(x, y)$ is defined by Eq. (6), and $\hat{\Sigma} = \hat{\Sigma}(x, y)$ denotes the self-energy due to the interaction that will be specified shortly. Subsequently, one can prove based on the gauge invariance that the equation for $\vec{\Psi}$ is also given in terms of \hat{G}_0 and $\hat{\Sigma}$ by^{4,6,15,16}

$$\int d^4y [\hat{G}_0^{-1}(x, y) - \hat{\Sigma}(x, y)] \hat{\sigma}_3 \vec{\Psi}(y) = \vec{0},$$

where $\hat{\sigma}_3$ originates from the asymmetry between $\psi_1 = \psi$ and $\psi_2 = \bar{\psi}$ under the gauge transformation. This equation may be written concisely by regarding x and y as matrix indices as

$$(\hat{G}_0^{-1} - \hat{\Sigma}) \hat{\sigma}_3 \vec{\Psi} = \vec{0}. \quad (13b)$$

Equation (13b) embodies “Goldstone’s theorem (I)” corresponding to the first proof,^{6,15} which is reduced for homogeneous systems to the Hugenholtz-Pines relation.³⁰ Unlike their original proof,³⁰ however, Eq. (13b) has been derived without imposing the 1PI condition on $\hat{\Sigma}$.^{4,6,15,16} Equation (13b) predicts a gapless excitation spectrum for \hat{G} . However, standard conserving approximations such as the Hartree-Fock-Bogoliubov theory fail to meet Eq. (13b), yielding an unphysical energy gap in the excitation spectrum.^{17,18}

Finally, the interaction energy $\langle S_{\text{int}} \rangle$ of Eq. (2b) can also be expressed in terms of \hat{G} and $\hat{\Sigma}$ as Eq. (12) of ref. 4; it reads in the present notation as

$$\begin{aligned} \langle S_{\text{int}} \rangle &= -\frac{1}{4} \sum_{ij} \int d^4x \int d^4y \Sigma_{ij}(x, y) \mathcal{G}_{ji}(y, x) \\ &\equiv -\frac{1}{4} \text{Tr} \hat{\Sigma} \hat{\mathcal{G}}, \end{aligned} \quad (14)$$

where $\hat{\mathcal{G}} = (\mathcal{G}_{ij})$ is a matrix composed of \hat{G} and $\vec{\Psi}$ as

$$\begin{aligned} \mathcal{G}_{ij}(x, y) &\equiv G_{ij}(x, y) + (-1)^i \Psi_i(x) \Psi^j(y) \\ &= [\langle T_\tau \psi_i(x) \psi^j(y) \rangle - 2\Psi_i(x) \Psi^j(y) \delta_{j,3-i}] (-1)^j. \end{aligned} \quad (15)$$

The second expression has been obtained by substituting Eq. (4b). Thus, each off-diagonal element of $\hat{\mathcal{G}}$ contains an extra term $2\Psi_i(x) \Psi^{3-i}(y) (-1)^i$ besides $\langle T_\tau \psi_i(x) \psi^j(y) \rangle (-1)^j$.

D. Effective action

Using \hat{G} and $\vec{\Psi}$, we formally express Γ of Eq. (11) for $\vec{J} = \vec{0}$ and $\hat{K} = \hat{0}$ in terms of another unknown functional $\Phi = \Phi[\vec{\Psi}, \hat{G}]$ as⁴

$$\begin{aligned} \Gamma[\vec{\Psi}, \hat{G}] &= \Gamma_0 - \frac{1}{2} \text{Tr} \vec{\Psi}^\dagger \hat{G}_0^{-1} \hat{\sigma}_3 \vec{\Psi} \\ &\quad + \frac{1}{2} \text{Tr} [\ln(\hat{1} - \hat{\Sigma} \hat{G}_0) + \hat{\Sigma} \hat{G}] + \beta \Phi[\vec{\Psi}, \hat{G}], \end{aligned} \quad (16)$$

where Γ_0 denotes contribution of non-interacting excitations from Eq. (2a), and $\hat{\Sigma} = \hat{\Sigma}[\vec{\Psi}, \hat{G}]$. Subsequently, we perform differentiations of Eq. (12) by using Eq. (13) and noting that $\vec{\Psi}^\dagger$ and $\vec{\Psi}$ in Eq. (16) yield the same contribution. Stationarity requirements of Eq. (12) are thereby transformed into a couple of conditions for Φ alone as

$$\beta \frac{\delta \Phi}{\delta G_{ji}(y, x)} = -\frac{1}{2} \Sigma_{ij}(x, y), \quad (17a)$$

$$\beta \frac{\delta \Phi}{\delta \Psi^i(x)} = \sum_j \int d^4y \Sigma_{ij}(x, y) (-1)^{j-1} \Psi_j(y). \quad (17b)$$

Action (16) for the normal-state limit of $(\Psi_i, G_{i,3-i}) \rightarrow (0, 0)$ is reduced to the Luttinger-Ward functional,^{1,4,8} where Φ is given as a power series of V_s with closed 2PI

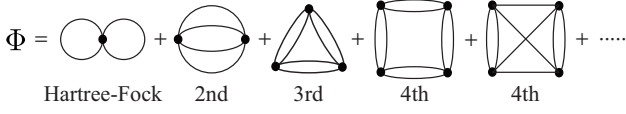


FIG. 1: Normal-state Φ drawn without arrows.

diagrams, i.e., those that cannot be separated by removing any pair of G lines. It may be expressed graphically as Fig. 1, where a filled circle denotes V_s of Eq. (7).

E. Identities in terms of Φ

Identity (14) for the interaction energy can be rephrased in terms of Φ . To see this, let us replace $V \rightarrow \lambda V$ in Eq. (2b) and differentiate the resultant $-\ln Z[\vec{0}, \hat{0}; \lambda]$ from Eq. (9) with respect to λ . Noting $(\partial/\partial\lambda)(\lambda V) = (\lambda V)/\lambda$, we obtain¹

$$-\frac{\partial \ln Z[\vec{0}, \hat{0}; \lambda]}{\partial \lambda} = \frac{\langle S_{\text{int}}(\lambda) \rangle}{\lambda} = -\frac{1}{4\lambda} \text{Tr} \hat{\Sigma}(\lambda) \hat{\mathcal{G}}(\lambda), \quad (18a)$$

where we have used Eq. (14) in the second equality. Subsequently, we replace $-\ln Z[\vec{0}, \hat{0}; \lambda]$ above by $\Gamma(\lambda)$ based on Eq. (11) and perform its differentiation with Eq. (16). Noting the stationarity conditions of Eq. (12), we only need to consider the explicit λ dependence in $\Gamma(\lambda)$ that lies in $\Phi(\lambda)$; see Fig. 1 for normal states on this point. Thus, we also obtain

$$-\frac{\partial \ln Z[\vec{0}, \hat{0}; \lambda]}{\partial \lambda} = \frac{\partial \Gamma(\lambda)}{\partial \lambda} = \beta \frac{\partial \Phi(\lambda)}{\partial \lambda}. \quad (18b)$$

Equating Eqs. (18a) and (18b) yields

$$\beta \frac{\partial \Phi(\lambda)}{\partial \lambda} = -\frac{1}{4\lambda} \text{Tr} \hat{\Sigma}(\lambda) \hat{\mathcal{G}}(\lambda). \quad (19)$$

Finally, we assume that $\Phi(\lambda)$ can be expanded from $\lambda = 0$ as

$$\Phi(\lambda) = \sum_{n=1}^{\infty} \lambda^n \Phi^{(n)}, \quad (20)$$

like the Luttinger-Ward functional for normal states given graphically as Fig. 1. Substituting Eqs. (17a) and (20) into Eq. (19), comparing terms of order λ^{n-1} , and setting $\lambda = 1$, we obtain an identity for $\Phi^{(n)}$ as

$$\begin{aligned} \Phi^{(n)} &= \frac{1}{2n} \sum_{ij} \int d^4x \int d^4y \frac{\delta \Phi^{(n)}}{\delta G_{ij}(x, y)} \mathcal{G}_{ij}(x, y) \\ &\equiv \frac{1}{2n} \text{Tr} \frac{\delta \Phi^{(n)}}{\delta \hat{G}} \hat{\mathcal{G}}. \end{aligned} \quad (21a)$$

Equation (17b) is also transformed by using Eq. (17a) into

$$\frac{\delta \Phi}{\delta \Psi^i(x)} = -2 \sum_j \int d^4y \frac{\delta \Phi}{\delta G_{ji}(y, x)} (-1)^{j-1} \Psi_j(y). \quad (21b)$$

These are the key identities corresponding to Eqs. (22) and (23) of ref. 4 that have been used to construct Φ . Indeed, the previous expressions are reproduced from Eq. (21) by writing $\Phi^{(n)}$ in terms of functions in Eq. (5) as $\Phi^{(n)}[\Psi, \bar{\Psi}, G, F, \bar{F}]$ and performing its differentiations. Equation (21a) is thereby transformed into

$$\begin{aligned} \Phi^{(n)} &= \frac{1}{2n} \int dx \int dy \left\{ \frac{\delta \Phi^{(n)}}{\delta G(x, y)} [G(x, y) - \Psi(x) \bar{\Psi}(y)] \right. \\ &\quad + \frac{\delta \Phi^{(n)}}{\delta F(x, y)} [F(x, y) - \Psi(x) \Psi(y)] \\ &\quad \left. + \frac{\delta \Phi^{(n)}}{\delta \bar{F}(x, y)} [\bar{F}(x, y) - \bar{\Psi}(x) \bar{\Psi}(y)] \right\}. \end{aligned} \quad (22a)$$

Equation (21b) for $i = 1$ also reads

$$\frac{\delta \Phi}{\delta \bar{\Psi}(x)} = - \int d^4y \left[\frac{\delta \Phi}{\delta G(y, x)} \Psi(y) + 2 \frac{\delta \Phi}{\delta \bar{F}(y, x)} \bar{\Psi}(y) \right]. \quad (22b)$$

These are exactly Eqs. (22) and (23) of ref. 4.

It is worth pointing out that expression (16) for Γ becomes exact when Φ satisfies Eq. (21a) at each order up to $n = \infty$. This can be shown in exactly the same way as for the normal state¹ with $V \rightarrow \lambda V$ in Eq. (2b) as follows. First, action $\Gamma(\lambda)$ obeys first-order differential equation (18b). Second, $\Gamma(\lambda)$ is identical with $-\ln Z[\vec{0}, \hat{0}; \lambda]$ at $\lambda = 0$, i.e., for the non-interacting case. Hence, we conclude that $\Gamma(\lambda) = -\ln Z[\vec{0}, \hat{0}; \lambda]$ holds true generally, especially for $\lambda = 1$. This completes the proof. Thus, the Φ -derivable scheme obeying Eq. (21a) includes the exact theory as a limit.

F. Procedure to construct $\Phi^{(n)}$

Difficulties in constructing $\Phi^{(n)}$ for BECs originate from anomalous interaction vertices of Fig. 2(b)-(d) that emerge upon condensation, which make the concept of “skeleton diagrams” introduced for normal states¹ obscure. To overcome them with avoiding any prejudice, inconsistency, or double counting, we have previously adopted the strategy of starting from the well-established normal-state Luttinger-Ward functional and successively incorporating contribution of all the diagrams characteristic of BECs so that either of identities (21a) and (21b) is satisfied. To this end, we have relaxed the conventional 2PI condition for Φ down to 1PI, considering that

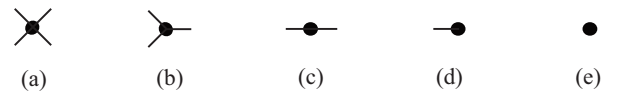


FIG. 2: Diagrammatic representation of the two-body interaction in terms of the excitation field $\psi'_i \equiv \psi_i - \langle \psi_i \rangle$. Each missing line in (b)-(e) compared with (a) corresponds to $\langle \psi_i \rangle$.

Φ obeying Eqs. (21a) and (21b) may not be found within the 2PI requirement.

The explicit procedure to construct Φ is summarized in terms of functions in Eq. (5) as (i)-(iv) below. See Figs. 3 and 4 for relevant diagrams of $n = 1$ and 2, respectively.

- (i) Draw all the normal-state diagrams contributing to $\Phi^{(n)}$, i.e., diagrams that appear in the Luttinger-Ward functional.¹ With each such diagram, associate the known weight of the normal state.
- (ii) Draw all the distinct diagrams obtained from those of (i) by successively changing directions of a pair of incoming and outgoing arrows at each vertex. This enumerates all the processes where F or \bar{F} characteristic of condensation is relevant in place of G . With each such diagram, associate an unknown weight c_ν .
- (iii) Draw all the distinct 1PI diagrams obtained from those of (i) and (ii) by successively removing a line, i.e., Green's function. This exhausts processes where the condensate wave function participates explicitly. The 1PI condition guarantees that the self-energies obtained by Eq. (17a) are composed of connected diagrams. Associate an unknown weight with each such diagram, except the one consisting only of a single vertex in the first order, i.e., the rightmost diagram in Fig. 3, for which the weight is easily identified to be $1/2\beta$. Indeed, the latter represents the term obtained from Eq. (2b) by replacing every field operator by its expectation value, i.e., the condensate wave function.
- (iv) Determine the unknown weights of (ii) and (iii) by requiring that either Eq. (22a) or (22b) be satisfied.

Now, we apply the above procedure to constructing $\Phi^{(1)}$. Its diagrams are enumerated in Fig. 3. The corresponding analytic expression is given by

$$\begin{aligned} \Phi^{(1)} = & \frac{1}{2\beta} \int dx' \int dy' \int dx \int dy V_s(x'y', xy) \\ & \times \{ 2G(x, x')G(y, y') + c_{2b}^{(1)} F(x, y)\bar{F}(x', y') \\ & + c_{1a}^{(1)} G(x, x')\Psi(y)\bar{\Psi}(y') + c_{1b}^{(1)} [F(x, y)\bar{\Psi}(x')\bar{\Psi}(y') \\ & + \bar{F}(x', y')\Psi(x)\Psi(y)] + \bar{\Psi}(x')\bar{\Psi}(y')\Psi(x)\Psi(y) \}. \end{aligned}$$

Introducing the rule of associating non-primed (primed) arguments with ψ ($\bar{\psi}$), we may express this $\Phi^{(1)}$ concisely as

$$\begin{aligned} \Phi^{(1)} = & \frac{1}{2\beta} \text{Tr} V_s [2GG + c_{2b}^{(1)} F\bar{F} + c_{1a}^{(1)} G\Psi\bar{\Psi} \\ & + c_{1b}^{(1)} (F\bar{\Psi}\bar{\Psi} + \bar{F}\Psi\Psi) + \bar{\Psi}\bar{\Psi}\Psi\Psi], \end{aligned} \quad (23a)$$

where GG , $F\bar{F}$, etc., are matrices with elements $G(x, y')G(y, x')$, $F(x, y)\bar{F}(x', y')$, etc. We now require that Eq. (22a) be satisfied, whose differentiations graphically correspond to removing a line of G , F , and \bar{F} from Fig. 3 in all possible ways, respectively. In this process, prefactors of Fig. 3(i) and (ii) with $2n$ ($n = 1$) Green's

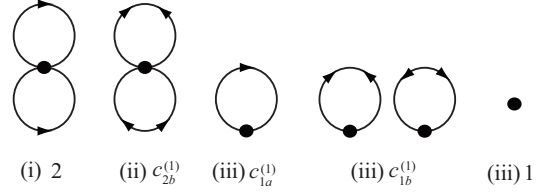


FIG. 3: Diagrams contributing to $\Phi^{(1)}$. A line with an arrow denotes G , and a line with two arrows signifies either F or \bar{F} as in the theory of superconductivity.²² Here (i)-(iii) distinguish three kinds of diagrams considered at different stages of the procedure given in the second paragraph of §II F, and numbers and unknown variables $c_\nu^{(1)}$ ($\nu = 2b, 1a, 1b$) denote relative weights of the diagrams. Each weight should be multiplied by $1/2\beta$ to obtain the absolute weight.

function lines vanish identically from the equation. This cancellation is characteristic of those diagrams with no condensate wave function and holds true order by order in Eq. (22a). Hence, Eq. (22a) for $n = 1$ is reduced to coupled algebraic equations for prefactors of latter three diagrams in Fig. 3, which read $c_{1a}^{(1)} = \frac{1}{2}(-2 \times 2 + c_{1a}^{(1)})$, $c_{1b}^{(1)} = \frac{1}{2}(-c_{2b}^{(1)} + c_{1b}^{(1)})$, $1 = \frac{1}{2}(-c_{1a}^{(1)} - 2c_{1b}^{(1)})$, respectively. Solving them, we obtain

$$c_{2b}^{(1)} = -1, \quad c_{1a}^{(1)} = -4, \quad c_{1b}^{(1)} = 1. \quad (23b)$$

It turns out that another identity (22b) with $\Phi \rightarrow \Phi^{(1)}$ also yields Eq. (23b).⁴ Thus, weights $c_\nu^{(1)}$ have been determined uniquely based on Eqs. (22a) and (22b).

Diagrams for $\Phi^{(2)}$ are enumerated in Fig. 4. Subsequently, we require that Eq. (22a) for $n = 2$ be satisfied, whose differentiations can also be performed graphically. The condition yields coupled algebraic equations originating from the prefactor for each diagram in Figs. 4 and 5. Those for the first row of Fig. 4 with $2n$ ($n = 2$) lines vanish identically, as mentioned earlier. On the other hand, equations for the second and third rows in Fig. 4

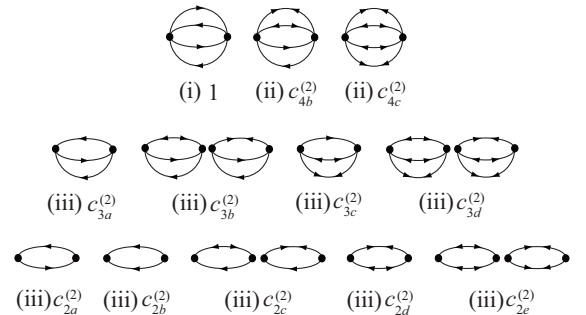


FIG. 4: Diagrams contributing to $\Phi^{(2)}$. Here (i)-(iii) distinguish three kinds of diagrams considered at different stages of the procedure given in the second paragraph of §II F, and number 1 and unknown weights $c_\nu^{(2)}$ ($\nu = 4b, \dots, 2e$) denote relative weights of these diagrams. Each weight should be multiplied by $-1/2\beta$ to obtain the absolute weight.



FIG. 5: Two kinds of extra diagrams relevant to the calculation of Eq. (22a) for $n = 2$.

and those for Fig. 5 are obtained as⁴

$$\begin{aligned} 0 &= c_{3a}^{(2)} + 4 = c_{3b}^{(2)} + c_{4b}^{(2)} = c_{3c}^{(2)} + 2c_{4b}^{(2)} = c_{3d}^{(2)} + 2c_{4c}^{(2)}, \\ 0 &= c_{2a}^{(2)} + c_{3a}^{(2)} + c_{3b}^{(2)} = 2c_{2b}^{(2)} + c_{3a}^{(2)} = 2c_{2c}^{(2)} + c_{3c}^{(2)} + 2c_{3b}^{(2)} \\ &= 2c_{2d}^{(2)} + c_{3c}^{(2)} + 4c_{3d}^{(2)} = 2c_{2e}^{(2)} + c_{3d}^{(2)}, \\ 0 &= c_{2a}^{(2)} + c_{2b}^{(2)} + c_{2c}^{(2)} = c_{2c}^{(2)} + c_{2d}^{(2)} + 2c_{2e}^{(2)}, \end{aligned}$$

respectively. Solving them, we obtain

$$\begin{aligned} c_{4b}^{(2)} &= -2, \quad c_{4c}^{(2)} = 1, \\ c_{3a}^{(2)} &= -4, \quad c_{3b}^{(2)} = 2, \quad c_{3c}^{(2)} = 4, \quad c_{3d}^{(2)} = -2, \\ c_{2a}^{(2)} &= c_{2b}^{(2)} = 2, \quad c_{2c}^{(2)} = -4, \quad c_{2d}^{(2)} = 2, \quad c_{2e}^{(2)} = 1. \end{aligned} \quad (24)$$

It turns out that another identity (22b) with $\Phi \rightarrow \Phi^{(2)}$ also yields Eq. (24).⁴

Thus, weights $c_\nu^{(2)}$ have been determined uniquely so as to satisfy both Eqs. (22a) and (22b). However, this has been possible only by relaxing the 2PI condition for Φ down to 1PI. Indeed, one may check easily by repeating the above calculation that $\Phi^{(2)}$ obeying either Eq. (22a) or (22b) cannot be found within the 2PI requirement of retaining only diagrams in the first and second rows of Fig. 4.

G. Discrepancy with the CJT formalism

Thus, the above analysis has shown that the Φ functional for BECs satisfying Eqs. (22a) and (22b) may only be constructed by including 1PI diagrams that lie outside the 2PI category. This conclusion has been reached based on a single requirement that Φ be expanded in terms of the interaction as Eq. (20) like the Luttinger-Ward functional. The condition also has been crucial for proving convergence of the series to the exact action, as given below Eq. (22b). However, the resultant Φ apparently contradicts the one obtained by CJT,¹² which consists of 2PI diagrams even for spontaneous broken-symmetry phases of $\langle \psi \rangle \neq 0$.

The proof by CJT for Φ being 2PI is based on the correspondence of Eq. (2.19) for $\Gamma(\phi, G)$ to Eq. (2.10) for $\Gamma(0, G)$,¹² with $\phi \rightarrow \vec{\Psi}$ and $G \rightarrow \hat{G}$ from their notation to ours. However, it may not be entirely clear in the context of Bose-Einstein condensation. First, $\Gamma(0, G)$ is relevant to normal states, so that the external source J^0 for $\phi = 0$ in Eq. (2.10) is necessarily equal to zero, i.e., the tadpole vertex of Fig. 2(d) is absent in $\Gamma(0, G)$. Thus, $\Gamma(0, G)$ is exactly the Luttinger-Ward functional of Fig. 1 that is composed only of the vertex of Fig. 2(a). On the other hand, $\Gamma(\phi, G)$ contains vertices of Fig. 2(b)-(d)

inherent in BECs besides the classical one of Fig. 2(e). The vertex of Fig. 2(c) has been removed by CJT to introduce another propagator \mathcal{D} with it, which reads in terms of Eqs. (6) and (7) in the present notation as

$$\begin{aligned} \hat{D}^{-1}(x, y) &\equiv \hat{G}_0^{-1}(x, y) - 2V_s(xy_1, yx_1)\Psi(x_1)\bar{\Psi}(y_1)\hat{\sigma}_3 \\ &\quad - V_s(xy, x_1y_1)\Psi(x_1)\Psi(y_1)\frac{\hat{\sigma}_1 + i\hat{\sigma}_2}{2} \\ &\quad + V_s(x_1y_1, xy)\bar{\Psi}(x_1)\bar{\Psi}(y_1)\frac{\hat{\sigma}_1 - i\hat{\sigma}_2}{2}, \end{aligned}$$

where integrations over repeated arguments (x_1, y_1) are implied. Thus, part of the interaction effects have been incorporated into the “bare” propagator \mathcal{D} .

However, it is not clear whether their 2PI series for $\phi \neq 0$ really converges to the exact Φ when collected up to the infinite order, due to the asymmetric treatment of interaction vertices in Fig. 2 as noted above. To be more specific, it does not obey Eq. (21a) at each order that has been crucial in proving the convergence for normal states¹ and also for BECs as given below the paragraph of Eq. (22b). Thus, the 2PI series may contain some over- or undercounting in the process of renormalization. Whether it converges to the exact action or not remains to be established. In this context, the CJT formalism has a difficulty that one may not find any approximate Φ that satisfies Eq. (13), as discussed by van Hees and Knoll,³⁴ who thereby proposed a further approximation $\tilde{\Gamma}[\vec{\Psi}] \equiv \Gamma[\vec{\Psi}, \hat{G}[\vec{\Psi}]]$ to meet Eq. (13b) alone.

III. OBTAINING Φ MORE CONCISELY

In this section, we will show that $\Phi[\vec{\Psi}, \hat{G}]$ may be simplified further to a functional of \hat{G} alone defined by Eq. (15). Given this is the case, we realize by noting $\delta\Phi^{(n)}[\hat{G}]/\delta\hat{G} = \delta\Phi^{(n)}[\hat{G}]/\delta\hat{G}$ that Eq. (21a) implies a manifest fact that every term in $\Phi^{(n)}$ is composed of $2n$ products of \mathcal{G}_{ij} . In addition, $\Phi[\hat{G}]$ automatically satisfies Goldstone’s theorem (I) given by Eq. (17b). This is shown by using Eqs. (15) and (17a), $\Psi^i(x) = \Psi_{3-i}(x)$, and $\Sigma_{ij}(x, y) = (-1)^{i+j-1}\Sigma_{3-j, 3-i}(y, x)$ as

$$\begin{aligned} \beta \frac{\delta\Phi[\hat{G}]}{\delta\Psi^i(x)} &= \sum_{j,k} \int d^4y \int d^4z \beta \frac{\delta\Phi[\hat{G}]}{\delta\mathcal{G}_{jk}(y, z)} \frac{\delta\mathcal{G}_{jk}(y, z)}{\delta\Psi^i(x)} \\ &= \sum_j \int d^4y \Sigma_{ij}(x, y) (-1)^{j-1} \Psi_j(y). \end{aligned} \quad (25)$$

Finally, a couple of requirements that (a) Φ be reduced to the Luttinger-Ward functional in the normal-state limit and (b) Φ be 1PI will be shown to determine $\Phi[\hat{G}]$ uniquely.

As a preliminary, let us define four functions in terms

of \mathcal{G}_{ij} in Eq. (15) by

$$\begin{aligned}\mathcal{G}(x, y') &\equiv \bar{\mathcal{G}}(y', x) \equiv \frac{\mathcal{G}_{11}(x, y') - \mathcal{G}_{22}(y', x)}{2} \\ &= G(x, y') - \Psi(x)\bar{\Psi}(y'),\end{aligned}\quad (26a)$$

$$\begin{aligned}\mathcal{F}(x, y) &\equiv \frac{\mathcal{G}_{12}(x, y) + \mathcal{G}_{12}(y, x)}{2} \\ &= F(x, y) - \Psi(x)\Psi(y),\end{aligned}\quad (26b)$$

$$\begin{aligned}\bar{\mathcal{F}}(x', y') &\equiv -\frac{\mathcal{G}_{21}(x', y') + \mathcal{G}_{21}(y', x')}{2} \\ &= \bar{F}(x', y') - \bar{\Psi}(x')\bar{\Psi}(y'),\end{aligned}\quad (26c)$$

in exactly the same way as Eq. (5). With these functions, an alternative procedure to construct $\Phi^{(n)}$ is summarized as follows:

- (i) Draw all the n th-order diagrams of the Luttinger-Ward functional. For each line with an arrow, associate G . Identify the weight w_j for each of them based on the normal-state Feynman rules.¹
- (ii) Add all the distinct “anomalous” diagrams characteristic of ODLRO that are obtained from those of (i) by successively changing directions of a pair of incoming and outgoing arrows at each vertex. For each line with an arrow (two arrows), associate G (F or \bar{F}). This exhausts processes where F or \bar{F} characteristic of condensation is relevant in place of G . With each such diagram, attach an unknown weight c_j .
- (iii) Write down $\Phi^{(n)}$ based on diagrams of (i) and (ii) with replacement $(G, F, \bar{F}) \rightarrow (\mathcal{G}, \mathcal{F}, \bar{\mathcal{F}})$.
- (iv) Determine the unknown weights of (ii) by requiring that $\Phi^{(n)}$ for $n \geq 2$ be 1PI, and $\Phi^{(1)}$ reproduce the classical diagram of Fig. 2(e) with the correct weight.

Deferring detailed consideration until $\Phi^{(3)}$, we first present results for $n = 1, 2$ obtained from the above procedure:

$$\Phi^{(1)} = \frac{1}{2\beta} \text{Tr} V_s (2\mathcal{G}\mathcal{G} - \mathcal{F}\bar{\mathcal{F}}), \quad (27)$$

$$\Phi^{(2)} = -\frac{1}{2\beta} \text{Tr} (V_s \mathcal{G}\bar{\mathcal{G}} V_s \mathcal{G}\bar{\mathcal{G}} - 2V_s \mathcal{G}\bar{\mathcal{G}} V_s \mathcal{F}\bar{\mathcal{F}} + V_s \mathcal{F}\bar{\mathcal{F}} V_s \mathcal{F}\bar{\mathcal{F}}). \quad (28)$$

It is straightforward to see that substitution of Eq. (26) into these expressions reproduces Eq. (23) for $\Phi^{(1)}$ and weights of Eq. (24) for $\Phi^{(2)}$. Note that diagrams needed here are the first two in Fig. 3 for $\Phi^{(1)}$, and those of the first row in Fig. 4 for $\Phi^{(2)}$.

Now, we consider $\Phi^{(3)}$ in detail. Here, distinct normal-state diagrams in process (i) above are the particle-hole and particle-particle bubble diagrams of Fig. 6(a) and (b), respectively, where a line with an arrow denotes G . The normal-state Feynman rules^{1,4} enable us to identify their relative weights unambiguously as $(w_{\text{ph}}, w_{\text{pp}}) = (4, 1)$ with a common factor $(3\beta)^{-1}$. Process (ii) yields

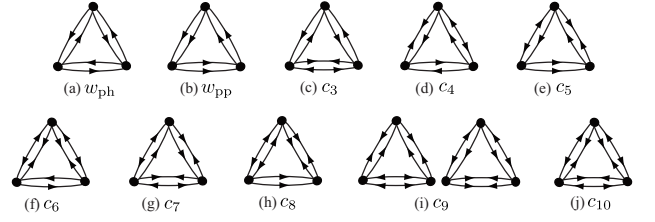


FIG. 6: Distinct diagrams for $\Phi^{(3)}$ with six G_{ij} lines.

diagrams (c)-(j) of Fig. 6, where a line with a pair of arrows toward (from) vertices denotes F (\bar{F}). Following process (iii) above, we express $\Phi^{(3)}$ analytically as

$$\begin{aligned}\Phi^{(3)} &= \frac{1}{3\beta} \text{Tr} [w_{\text{ph}} V_s \mathcal{G}\bar{\mathcal{G}} V_s \mathcal{G}\bar{\mathcal{G}} V_s \mathcal{G}\bar{\mathcal{G}} + w_{\text{pp}} V_s \mathcal{G}\mathcal{G} V_s \mathcal{G}\mathcal{G} V_s \mathcal{G}\mathcal{G} \\ &\quad + c_3 V_s \mathcal{G}\bar{\mathcal{G}} V_s \mathcal{G}\bar{\mathcal{G}} V_s \mathcal{F}\bar{\mathcal{F}} + c_4 V_s \mathcal{G}\bar{\mathcal{F}} V_s \mathcal{G}\mathcal{F} V_s \mathcal{G}\bar{\mathcal{G}} \\ &\quad + c_5 V_s \mathcal{G}\mathcal{F} V_s \mathcal{G}\bar{\mathcal{F}} V_s \mathcal{G}\mathcal{G} + c_6 V_s \mathcal{F}\bar{\mathcal{F}} V_s \mathcal{F}\bar{\mathcal{F}} V_s \mathcal{G}\bar{\mathcal{G}} \\ &\quad + c_7 V_s \bar{\mathcal{G}} \mathcal{F} V_s \bar{\mathcal{G}} \bar{\mathcal{F}} V_s \mathcal{F}\bar{\mathcal{F}} + c_8 V_s \mathcal{F}\mathcal{F} V_s \bar{\mathcal{F}} \bar{\mathcal{F}} V_s \mathcal{G}\mathcal{G} \\ &\quad + c_9 (V_s \bar{\mathcal{G}} \bar{\mathcal{F}} V_s \mathcal{G}\bar{\mathcal{F}} V_s \mathcal{F}\mathcal{F} + V_s \mathcal{G}\mathcal{F} V_s \bar{\mathcal{G}} \mathcal{F} V_s \bar{\mathcal{F}} \bar{\mathcal{F}}) \\ &\quad + c_{10} V_s \mathcal{F}\bar{\mathcal{F}} V_s \mathcal{F}\bar{\mathcal{F}} V_s \mathcal{F}\bar{\mathcal{F}}],\end{aligned}\quad (29a)$$

where $\mathcal{G}\bar{\mathcal{G}}$, $\mathcal{F}\bar{\mathcal{F}}$, etc., are matrices with elements $\mathcal{G}(x, y')\bar{\mathcal{G}}(x', y)$, $\mathcal{F}(x, y)\bar{\mathcal{F}}(x', y')$, etc., with $\mathcal{G}\bar{\mathcal{G}}$ and $\mathcal{G}\mathcal{G}$ denoting the particle-hole and particle-particle bubbles, respectively. This $\Phi^{(3)}$ generally contains non-1PI diagrams due to the contribution of the condensate wave functions in Eq. (26). The leading ones among them are those of Fig. 7 with three G_{ij} lines. Following process (iv), we require that their contribution vanish identically. Figure 7(a), for example, is derivable from Fig. 6(a), (c), and (d) by removing three lines adequately, and numbers of the combinations are easily identified as 6, 2, and 1, respectively. Thus, the requirement that Fig. 7(a) vanish yields $6w_{\text{ph}} + 2c_3 + c_4 = 0$. The same consideration for every diagram of Fig. 7 provides: (a) $6w_{\text{ph}} + 2c_3 + c_4 = 0$, (b) $6w_{\text{pp}} + c_5 = 0$, (c) $2c_3 + c_4 + 2c_6 = 0$, (d) $c_5 + 2c_8 = 0$, (e) $c_4 + 2c_9 = 0$, (f) $c_4 + c_5 = 0$, (g) $c_4 + 2c_5 + c_7 = 0$, (h) $c_5 + c_7 = 0$, (i) $c_4 + c_7 + 4c_9 = 0$, (j) $c_7 + 2c_9 = 0$, (k) $2c_3 + 2c_6 + c_7 = 0$, (l) $2c_8 + 2c_9 = 0$, (m) $2c_6 + c_7 + 6c_{10} = 0$, (n) $2c_8 + 2c_9 = 0$. They can be solved uniquely in terms

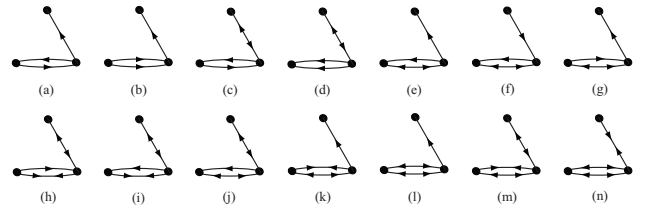


FIG. 7: Leading non-1PI diagrams for $\Phi^{(3)}$ whose contribution should vanish. Each diagram has its partner obtained by inverting all the arrows simultaneously.

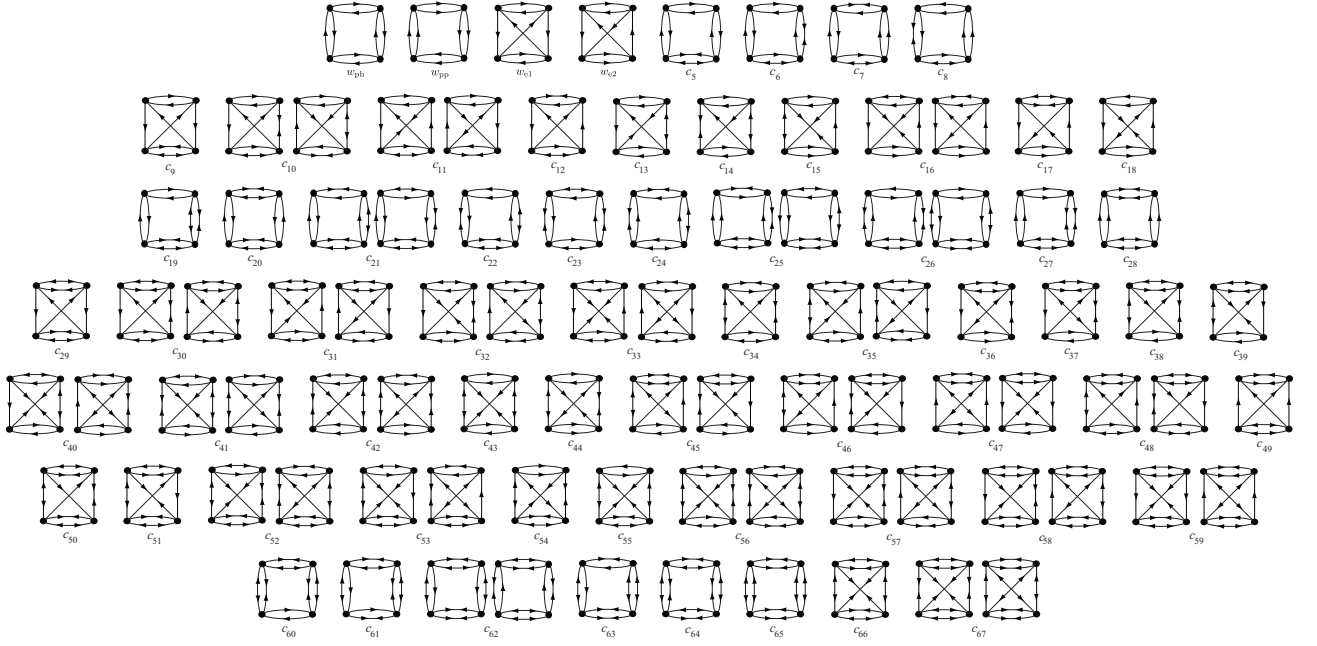


FIG. 8: Diagrams for $\Phi^{(4)}$ with eight G_{ij} lines. The first four survive in the normal state, whose relative weights are found to be $(w_{\text{ph}}, w_{\text{pp}}, w_{\text{e1}}, w_{\text{e2}}) = (8, 1, 16, 16)$ with the common factor $-(4\beta)^{-1}$. The 1PI requirement for $\Phi^{(4)}[\hat{\mathcal{G}}]$ determines weights c_j ($j = 5, \dots, 67$) of the anomalous diagrams uniquely as $4w_{\text{ph}} = c_{19} = 2c_{20} = 4c_{64}$, $8w_{\text{pp}} = -c_6 = c_7 = -c_8 = -c_{12} = c_{16} = -2c_{18} = -c_{21} = c_{22} = c_{23} = c_{24} = -c_{25} = 2c_{26} = 2c_{27} = 4c_{28} = -c_{32} = -2c_{33} = -c_{34} = -c_{35} = c_{42} = -2c_{46} = c_{48} = -4c_{49} = -2c_{56} = c_{57} = -c_{61} = 2c_{62} = -c_{63} = 8c_{65} = -8c_{67}$, $4w_{\text{e1}} = c_{39} = 4c_{43} = 2c_{50}$, $2w_{\text{e2}} = -c_{11} = -c_{30} = c_{36} = -c_{41} = 2c_{44} = 2c_{45} = -c_{53} = 2c_{59}$, $-4w_{\text{ph}} + 4w_{\text{pp}} = c_5 = c_{60}$, $8w_{\text{pp}} + 2w_{\text{e2}} = c_{10} = -c_{15} = -2c_{17} = c_{31} = c_{40} = -2c_{47} = c_{52} = -2c_{54} = -2c_{58}$, $-8w_{\text{pp}} - 4w_{\text{e1}} - 2w_{\text{e2}} = 2c_9 = c_{13} = c_{38} = c_{51} = 2c_{55}$, $8w_{\text{pp}} + 4w_{\text{e1}} + 4w_{\text{e2}} = 2c_{14} = 4c_{29} = c_{37} = 4c_{66}$.

of normal-state weights $(w_{\text{ph}}, w_{\text{pp}}) = (4, 1)$ as

$$\begin{aligned} c_3 &= 3c_{10} = -3(w_{\text{ph}} + w_{\text{pp}}), \\ c_4 &= -c_5 = c_7 = 2c_8 = -2c_9 = 6w_{\text{pp}}, \\ c_6 &= 3w_{\text{ph}}. \end{aligned} \quad (29b)$$

The solution also removes all the other non-1PI diagrams with less than three G_{ij} lines from $\Phi^{(3)}$, as may be confirmed easily. Expression (29) with $(w_{\text{ph}}, w_{\text{pp}}) = (4, 1)$ coincides exactly with that obtained previously in terms of \hat{G} and $\hat{\Psi}$; see Appendix B of ref. 4. Looking back at Eq. (29b), we also realize that each normal-state diagram of Fig. 6(a) and (b) can independently be a source of an approximate Φ for BECs that satisfies both Noether's theorem and Goldstone's theorem (I), i.e., we can find an approximate Φ from Fig. 6(a) alone by setting $(w_{\text{ph}}, w_{\text{pp}}) = (4, 0)$ or from Fig. 6(b) alone by choosing $(w_{\text{ph}}, w_{\text{pp}}) = (0, 1)$.

To confirm the validity of our procedure, we have extended our consideration to the 4th order. The results are summarized in Fig. 8 and its caption. The relevant normal-state diagrams in the 4th order are the



FIG. 9: Leading non-1PI diagrams of the 4th order drawn without arrows.

first four diagrams of Fig. 8, whose relative weights are found as $(w_{\text{ph}}, w_{\text{pp}}, w_{\text{e1}}, w_{\text{e2}}) = (8, 1, 16, 16)$. The requirement that “all the leading non-1PI diagrams of Fig. 9 vanish” has been confirmed to determine all the weights of anomalous diagrams uniquely in terms of $(w_{\text{ph}}, w_{\text{pp}}, w_{\text{e1}}, w_{\text{e2}})$. The fact also implies that each of the first-four normal-state diagrams in Fig. 8 can independently be a source for an approximate Φ that satisfies both Noether's theorem and Goldstone's theorem (I).

IV. SUMMARY

We have developed a concise procedure to construct the effective action for BECs in such a way that both Noether's theorem and Goldstone's theorem (I) are satisfied at each order of a power series in terms of the interaction. It is found that every normal-state diagram can be a source of an approximate Φ for BECs. However, this is found possible only at the 1PI level instead of 2PI due to the anomalous structures of the bare interaction vertices as shown in Fig. 2. The resultant self-energy, obtained by Eq. (17a), should necessarily be one-particle reducible (1PR); this structure has been overlooked and may change our standard understanding of BECs substantially. For example, leading non-2PI diagrams for Φ in the dilute limit is given by the series of Fig. 10. They are predicted to modify the Lee-Huang-

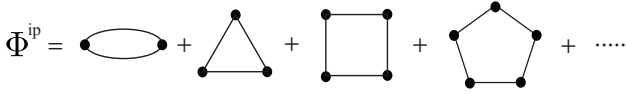


FIG. 10: Approximate series Φ^{ip} dominant in the dilute limit.

Yang expression²¹ for the ground-state energy per particle into²⁷

$$\frac{E}{N} = \frac{2\pi\hbar^2 an}{m} \left[1 + \left(\frac{128}{15\sqrt{\pi}} + \frac{16}{5} c_{\text{ip}} \right) \sqrt{a^3 n} \right], \quad (30)$$

where a and n are the s -wave scattering length and particle density, respectively, and $c_{\text{ip}} = O(1)$ is an additional constant due to Φ^{ip} . Moreover, this contribution is expected to change the nature of poles of \hat{G} , which domi-

nate thermodynamic properties of dilute BECs, from the Bogoliubov mode with an infinite lifetime²⁰ into a bubbling mode with a large decay rate proportional to a ,²⁸ instead of a^2 for the normal state. However, the fact does not contradict “Goldstone’s theorem (II)” from the second proof based on the commutation relation,^{6,15} which predicts a gapless mode with an infinite lifetime for homogeneous systems. As shown previously,¹⁹ Goldstone’s theorem (II) is relevant to three-point functions for BECs sharing poles with four-point functions, where the 1PR structure cancels out to yield an infinite lifetime for the collective excitations. Thus, their poles are distinct from those of \hat{G} .²⁹ The fact illustrates that the contents of the two proofs^{6,15} are not identical in general and should be distinguished clearly as “Goldstone’s theorem (I)” and “Goldstone’s theorem (II).”¹⁹

- ¹ J. M. Luttinger and J. C. Ward, Phys. Rev. **118**, 1417 (1960).
- ² C. De Dominicis and P. C. Martin, J. Math. Phys. **5**, 14 (1964).
- ³ N. E. Bickers and D. J. Scalapino, Ann. Phys. (NY) **193**, 206 (1989).
- ⁴ T. Kita, Phys. Rev. B **80**, 214502 (2009).
- ⁵ T. Kita, J. Phys. Soc. Jpn. **80**, 124704 (2011).
- ⁶ S. Weinberg, *The Quantum Theory of Fields II* (Cambridge Univ. Press, Cambridge, 1996).
- ⁷ L. P. Kadanoff and G. Baym, *Quantum Statistical Mechanics* (Benjamin, New York, 1962).
- ⁸ G. Baym, Phys. Rev. **127**, 1391 (1962).
- ⁹ J. Schwinger, J. Math. Phys. **2**, 407 (1961).
- ¹⁰ L. V. Keldysh, Zh. Eksp. Teor. Fiz. **47**, 1515 (1964) [Sov. Phys. JETP **20**, 1018 (1965)].
- ¹¹ T. Kita, Prog. Theor. Phys. **123**, 581 (2010).
- ¹² J. M. Cornwall, R. Jackiw, and E. Tomboulis, Phys. Rev. D **10**, 2428 (1974).
- ¹³ J. Knoll, Y. B. Ivanov, and D. Voskresensky, Ann. Phys. (N.Y.) **293**, 126 (2001).
- ¹⁴ J. Berges, Nucl. Phys. A **699**, 847 (2002).
- ¹⁵ J. Goldstone, A. Salam, and S. Weinberg, Phys. Rev. **127**, 965 (1962).
- ¹⁶ G. Jona-Lasinio, Nuovo Cimento **34**, 1790 (1964).
- ¹⁷ P. C. Hohenberg and P. C. Martin, Ann. Phys. (N.Y.) **34**, 291 (1965).
- ¹⁸ A. Griffin, Phys. Rev. B **53**, 9341 (1996).

- ¹⁹ T. Kita, J. Phys. Soc. Jpn. **80**, 084606 (2011).
- ²⁰ N. N. Bogoliubov, J. Phys. (USSR) **11**, 23 (1947).
- ²¹ T. D. Lee, K. Huang, and C. N. Yang, Phys. Rev. **106**, 1135 (1957).
- ²² A. A. Abrikosov, L. P. Gorkov, and I. E. Dzyaloshinski, *Methods of Quantum Field Theory in Statistical Physics* (Prentice Hall, Englewood Cliffs, N.J., 1963).
- ²³ J. Gavoret and P. Nozières, Ann. Phys. **28**, 349 (1964).
- ²⁴ P. Szépfalusy and I. Kondor, Ann. Phys. (N.Y.) **82**, 1 (1974).
- ²⁵ V. K. Wong and H. Gould, Ann. Phys. (N.Y.) **83**, 252 (1974).
- ²⁶ A. Griffin, *Excitations in a Bose-Condensed Liquid* (Cambridge University Press, Cambridge, 1993).
- ²⁷ K. Tsutsui and T. Kita, J. Phys. Soc. Jpn. **82**, 063001 (2013).
- ²⁸ K. Tsutsui and T. Kita, J. Phys. Soc. Jpn. **83**, 033001 (2014).
- ²⁹ T. Kita, Phys. Rev. B **81**, 214513 (2010).
- ³⁰ N. M. Hugenholtz and D. Pines, Phys. Rev. **116**, 489 (1959).
- ³¹ A. Altland and B. Simons: *Condensed Matter Field Theory* (Cambridge Univ. Press, Cambridge, 2010).
- ³² C. N. Yang, Rev. Mod. Phys. **34**, 694 (1962).
- ³³ S. T. Beliaev, Zh. Eksp. Teor. Fiz. **34**, 417 (1958) [Sov. Phys. JETP **7**, 289 (1958)].
- ³⁴ H. van Hees and J. Knoll, Phys. Rev. D **66**, 025028 (2002).